TELKOMNIKA, Vol.17, No.1, February 2019, pp.463~472
ISSN: 1693-6930, accredited First Grade by Kemenristekdikti, Decree No: 21/E/KPT/2018
DOI: 10.12928/TELKOMNIKA.v17i1.11604

Classification of neovascularization using convolutional neural network model

Wahyudi Setiawan[1], Moh. Imam Utoyo[2], Riries Rulaningtyas[*3]
[1]Informatics Department, University of Trunojoyo Madura, Bangkalan, Indonesia
[1,2]Mathematics Department, University of Airlangga, Surabaya, Indonesia
[3]Physics Department, University of Airlangga, Surabaya, Indonesia
*Corresponding author, e-mail: riries-r@fst.unair.ac.id

Abstract

Neovascularization is a new vessel in the retina beside the artery-venous. Neovascularization can appear on the optic disk and the entire surface of the retina. The retina categorized in Proliferative Diabetic Retinopathy (PDR) if it has neovascularization. PDR is a severe Diabetic Retinopathy (DR). An image classification system between normal and neovascularization is here presented. The classification using Convolutional Neural Network (CNN) model and classification method such as Support Vector Machine, k-Nearest Neighbor, Naïve Bayes classifier, Discriminant Analysis, and Decision Tree. By far, there are no data patches of neovascularization for the process of classification. Data consist of normal, New Vessel on the Disc (NVD) and New Vessel Elsewhere (NVE). Images are taken from 2 databases, MESSIDOR and Retina Image Bank. The patches are made from a manual crop on the image that has been marked by experts as neovascularization. The dataset consists of 100 data patches. The test results using three scenarios obtained a classification accuracy of 90%-100% with linear loss cross validation 0%-26.67%. The test performs using a single Graphical Processing Unit (GPU).

Keywords*: classification, convolutional neural network, deep learning, diabetic retinopathy, neovascularization.*

1. Introduction

Fundus image is a retinal image obtained from the fundus camera. An expert analyzes the fundus image to determine retina diseases. Diabetic Retinopathy (DR) is one of the retinal diseases. Usually, DR is present on Diabetes Mellitus (DM) patient for more than 15 years. DR causes blindness if not treated early [1].

A study in the UK, from 2004 to 2014, reported the number of people with DR. The study used a sample of 7,707,475 DM patients. The results showed a percentage of DR sufferers increases every year. In 2004, the number of patients with DR 0.9%, in 2014 increased to 2.3% of the DM patients [2]. Other studies, the people with DR in Southeast Asia, reported 35% of patients with DM [3].

Clinical examination of DR is done through several tests include biomicroscope, fluorescein angiography, fundus photo, and indocyanine green angiography. Also, experts perform Optical Coherence Tomography (OCT). The results of the analysis should be supported by age-related information, medical history, visual acuity, cardiovascular and disease progression [4, 5]. The examination procedures consist of several tests. It needs a relatively long time and expensive cost. An alternative solution is DR computationally detection.

The degree of abnormality DR is Non-Proliferative Diabetic Retinopathy (NPDR) and Proliferative Diabetic Retinopathy (PDR). This article has focused on PDR classification. The symptoms of PDR are new blood vessels on the surface of the retina or new blood vessels in the Optic Disk. Figure 1 shows PDR fundus images.

There is widely research on PDR. Jelinek et al. have classified NPDR and PDR [6]. Goatman et al. have classified two classes, normal and abnormal [7]. Akram *et al.* have classified three classes, normal, NVD, and NVE [8]. Welikala *et al.* have classified two classes, PDR and NPDR [9]. Gupta *et al.* have classified three classes, NVE, NPDR and Normal [10].

The study performs image processing with conventional method phases. It includes preprocessing, segmentation, feature extraction, feature selection, and classification. The

Received June 10, 2018; Revised November 9, 2018; Accepted December 7, 2018

feature extraction is done manually. The features appropriate for the classification process. In addition to conventional methods, the ability to perform classification is limited in the number of classes.

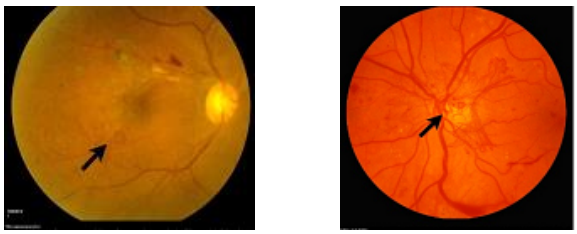

(a) (b)

Figure 1. (a) New vessel elsewhere, (b) New Vessel on the disc. data from retina image bank

Currently, there has been growing research on deep learning. Deep learning can be utilized in image processing. Research on the image classification using deep learning has been widely generated. The study about Deep Learning classification on diabetic retinopathy has been developed. Pratt et al. classified five classes from the DR level. DR levels are no DR, Mild DR, Moderate DR, Severe DR, and PDR. Data using 80,000 for training and 5,000 for validation of Kaggle dataset. CNN architecture consists ten convolution layers and three fully connected layer. The input data size is 512x512 pixel. It is used preprocessing with color normalization. The experimental results obtained accuracy 75%, specificity 95%, sensitivity 30% [11] .

Lee et al. classified two classes of normal and Age-related Macular Degeneration (AMD). The data used is OCT photos. The data consisted of 52,690 normal and 48,312 AMD. The method used is CNN with a modified VGG16 model. The system consists of 13 layers of convolution, and 3 Fully Connected Layer (FCL). The results showed an accuracy of 87.63% to 93.45% [12].

Takahashi et al. classified three classes of DR. Levels of DR are Simple Diabetic Retinopathy (SDR), Pre-Proliferative DR (PPDR) and PDR. Data consists of 9,939 fundus images from 2,740 patients. Modified GoogLeNet is applied for the classification test. Modified GoogLeNet uses crop image size 1272x1272 pixel and 4 batch size reduction. This research obtained accuracy 81% [13].

Lam et al. proposed the classification of lesions on the fundus. There are 5 classes of hemorrhages, microaneurysms, exudates, neovascularization and normal. The data from kaggle dataset consists of 1324 patches, 243 images. Validation uses an eOphta dataset composed of 148 patches microaneurysms and 47 patches exudates. Methods using CNN with AlexNet, VGG16, GoogleNet, ResNet and Inception-V3 models. The results show an accuracy of 74% to 96% [14].

Research on the specific classification of neovascularization using deep learning has not been done. Classification of two classes includes NVE & NVD. Until now, the classification was recognized the grade of DR. Research has not achieved maximum accuracy, so there is still a chance to get better accuracy.

This paper proposes a classification of fundus image for normal and neovascularization. The method was the CNN model include AlexNet, VGG16, VGG19, ResNet50, and GoogLeNet. It also using classification method include Support Vector Machine (SVM), Naïve Bayes Classifier (NBC), k-Nearest neighbor (k-NN), Discriminant Analysis, and Decision Tree. Data was taken form MESSIDOR and Retina Image Bank. Data was an RGB image without any pre-processing method. Experiments were carried out on a single Graphical Processing Unit (GPU).

2. Research Method

2.1. Deep Learning

Deep learning is part of machine learning. Deep learning can be applied to big data. Deep learning is capable of performing supervised and unsupervised learning. Deep learning

consists of many nonlinear layers. Usefulness of deep learning such as for pattern analysis and classification. The data analyzed can be image, text, and sound. Deep Learning methods i.e. the Convolutional Neural Network (CNN), Deep Belief Network (DBN), Stack Auto Encoder (SAE) and Convolutional Auto Encoder (CAE) [15-17].

2.2. Convolutional Neural Network

Convolutional Neural Network (CNN) is a method of Deep Learning. CNN is usually used for classification, segmentation and image analysis. The CNN architecture has several layers. The Layer consists of the convolution layer with the size of stride and zero padding, max pooling layer and fully connected layer. The study used an AlexNet model which has 25 layers [18]. Figure 2 show CNN fundus pipeline.

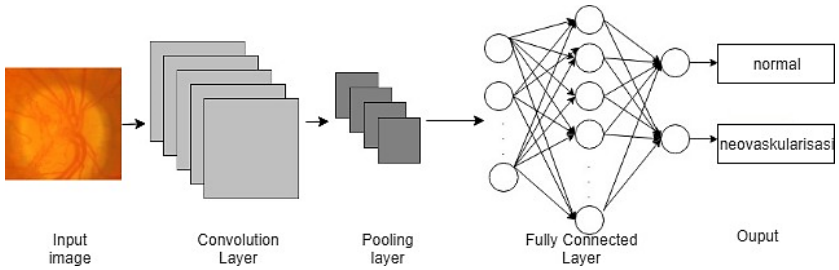

Figure 2. CNN fundus pipeline

2.2.1. Convolution Layers

Convolution is the multiplication operation between the input matrix and the filter matrix. Commonly filters used include identity operations, edge detection, sharpen, blur box and Gaussian blur. The convolution process between input matrix and filter are shown in Figure 3 [19].

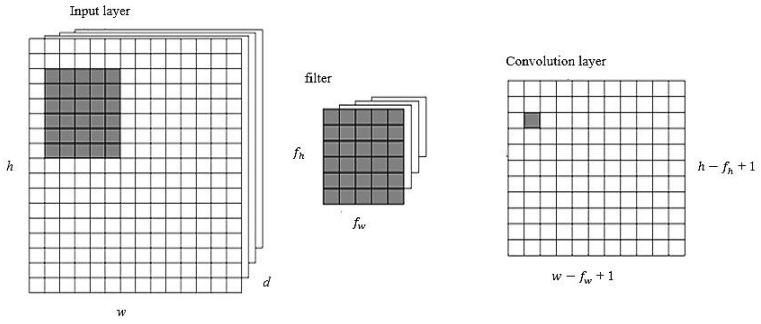

Figure 3. Input layer, filter and convolution layer

The Convolution process includes input layer, filter, and convolution layer. Volume dimension input, filter dimension and volume dimension output show in (1–3).

$$V_{input} = h \times w \times d \quad (1)$$

here, image matrix: h = heigh; w = width; d = dimension; V_{input} = volume dimension input

$$f = f_h \times f_d \quad (2)$$

filter matrix: f = filter ; f_h = filter of high; f_d = filter of dimension

$$V_{output} = (h - f_h + 1)\, x\, (f - f_w + 1) \times 1 \quad (3)$$

convolution layer: V_{output} = volume dimension output

2.2.2. Stride

Stride is the number of shifts made during the convolution process in the image matrix. If the value is stride 1, then the convolution process shifts 1 pixel. If the value of the value of stride 2, then the process of convolution shifted 2 pixels and so on. Shifts can occur both horizontally and vertically [20]. Illustration of stride 2 horizontal is shown in Figure 4, matrix shifts horizontally.

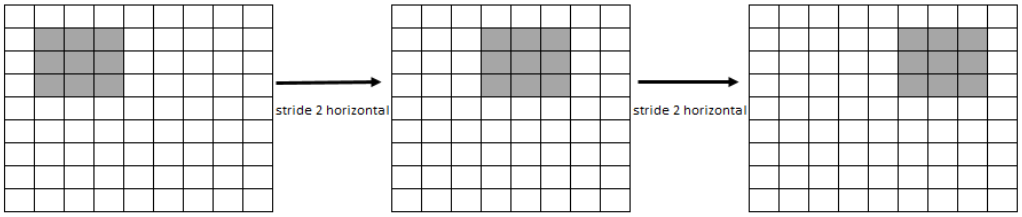

Figure 4. Stride 2 horizontal

2.2.3. Padding

Padding is done when the image matrix does not match the filter matrix size. Usually occurs when doing convolution on the edge of the image. There are two options [20] :

1. Fixed in a condition of image matrix value called valid padding
2. Replace the value in the image matrix with zero (zero padding). Zero padding of size 2 is shown in Figure 5.

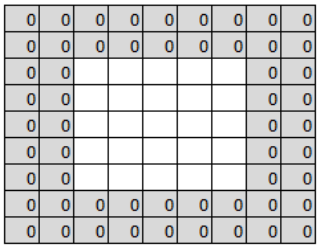

Figure 5. Zero padding of size 2

2.2.4. ReLU

Rectified Linear Unit (ReLU) is a step to change the output. If the output is negative then, ReLU will convert it to zero. The output of ReLU shown in (4) [19]. ReLU operation is shown in Figure 6. A negative value on matrix become zero.

$$f(x) = \max\ (0, x) \tag{4}$$

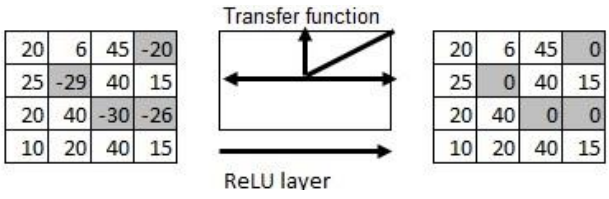

Figure 6. ReLU operation

2.2.5. Pooling layer

Pooling layer is a layer that reduces the image dimension matrix. Spatial pooling has 3 types of max-pooling, average-pooling, and sum-pooling. Max-pooling is the common used of special pooling [21]. Max Pooling operation is shown in Figure 7.

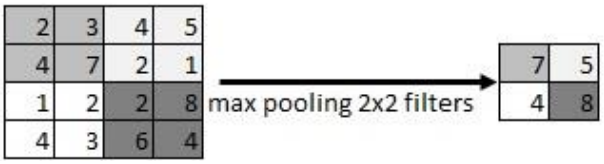

Figure 7. Max pooling

2.2.6. Fully Connected Layer

Fully Connected Layer (FCL) is a layer similar to a neural network. The input of FCL is the image features converted to vector. Furthermore, the activation function will classify the test image as a specific class image. FCL is the final learning phase that functions as a classification [22].

2.2.7. Dropout

Dropout is a control for the overfitting process on a neural network. Overfitting occurs when the system takes all features including noise. Dropout stage is very simple and can be useful to handle overfitting problems [23]. In the dropout layer, the options for the dropout unit are done randomly. The dropout illustration is shown in Figure 8.

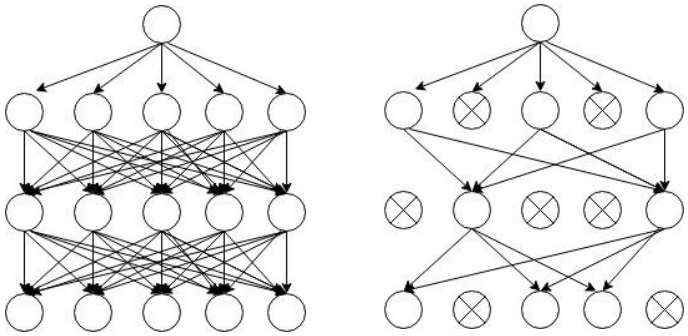

(a) (b)

Figure 8. (a) Standard Neural Net, (b) Applying Dropout

2.2.8. Softmax

Softmax is done in the final stages of FCL. Softmax works like an activation layer. Softmax is used in multiclass classification. Softmax generates probability values for each class. The highest probability value indicates the class of the object input [21]. The activation function of softmax shown in (5).

$$\sigma(a_j) = \frac{exp^{a_j}}{\sum_{k=1}^{m} \exp a_k} \quad (5)$$

here, $a = [a_1, \ldots, a_m]^T$ is a vector with m elements. We can check that $\sum_{j=1}^{m} \sigma\,(a_j) = 1$ for softmax.

2.2.9. System Architecture

System Architecture using AlexNet 25-layer model. The model consists of 5-layer convolutions each measuring 11x11, 5x5, and three 3x3-sized convolution layers. Layer convolution is done by stride and padding process. Among the layer's convolutions are ReLU, Normalization and Max Pooling. Next 2 Fully Connected Layer with ReLU, Max Pooling and Dropout 0.5. In the end, there is a Fully Connected Layer with Softmax. The output will classify the two classes of Normal and Neovascularization [18]. The system architecture is shown in Figure 9.

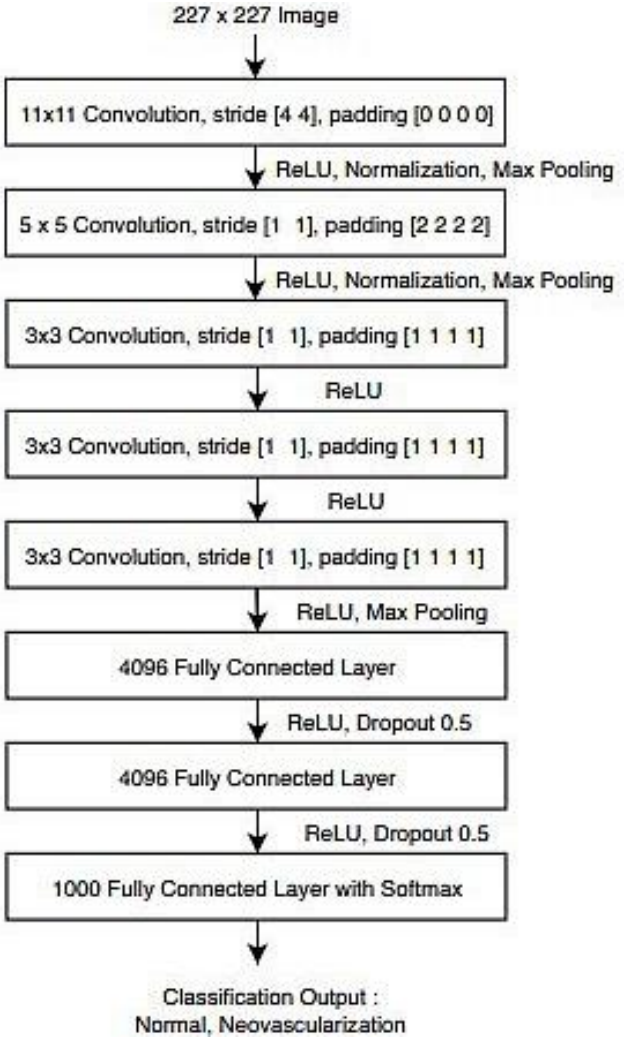

Figure 9. System architecture

Another CNN models that used in the experiment are VGG16, VGG19 [24], ResNet50 [25], and GoogleNet [26]. The models consist of 41, 47, 177, and 144 layers. The difference between AlexNet and another CNN models are image input size, type, and sequence of the layer. AlexNet have 227x227 image input size, another CNN models have 224x224. FCL in Alexnet, VGG16, VGG19 is 'fc7'. FCL in ResNet50 is 'fc1000'. FCL in GoogLeNet is 'loss3-classifier'.

2.3. Data Acquisition

The data acquisition is from the public database of MESSIDOR and Retina Image Bank. The MESSIDOR has been commonly used as a classification and analysis of diabetic retinopathy. However, the number of neovascularization images is relatively small from the total number of 1,200 available. The MESSIDOR dataset can be accessed via http://www.adcis.net/en/Download-Third-Party/Messidor.html [27]. While Retina Image Bank is a fundus data set made by the American Society of Retina Specialist. In Retina Image Bank dataset there are 23,650 image fundus data. The fundus is accompanied by a description of various disorders of retinal disease including neovascularization. Retina Image Bank dataset can be accessed via http://imagebank.asrs.org/home.

The testing data consist of patches. Patches obtained through manual cropping of images on the optic disk and other retinal surfaces. Figure 10 shows the neovascularization patches that used in this research.

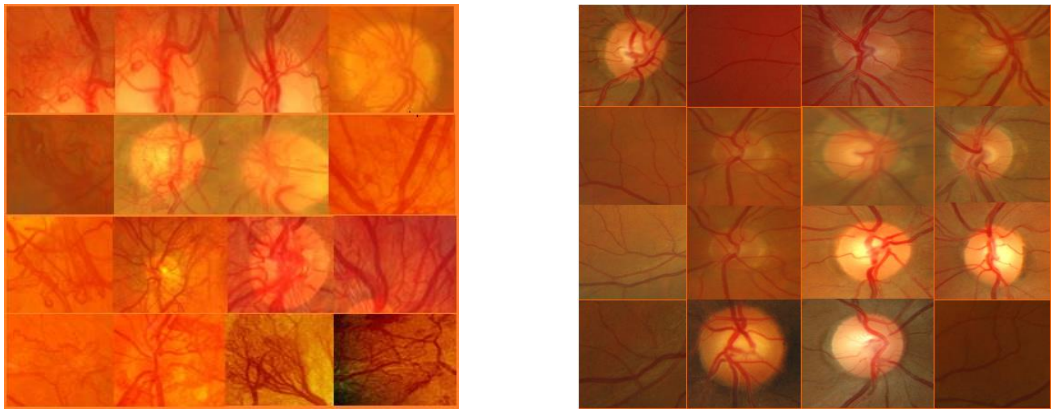

(a) (b)

Figure 10. (a) Representative of neovascularization patches, (b) Normal patches

2.4. Implementation

The stages of implementation are explained below:

1. Prepare a dataset consisting of normal images and neovascularization. Perform manual cropping to get patches of images on the optic disc and other retinal surfaces.
2. Normalize the patches size to 227x227 pixel. The pixel size is the default of the AlexNet input layer.
3. Determine the type and number of layers used in the CNN architecture. The type and number of layers used in this study are shown in Figure 9.
4. Determine the number of patches used for the training process. If the number of images in the datastore is greater than the amount of training data used, the system selects random patches used for the training process.
5. Conduct training data labeling. Labeling will look as follows:
   [[The array of patches], [label of normal or neovascularization]]
6. Feature extraction from the training dataset. Feature extraction is found in the activation process. Specify the ReLU activation layer used for feature extraction. ReLU is on the 7th layer of the CNN architecture used.
7. Determine the amount of data in the testing process.
8. Perform feature extraction on dataset testing. The feature extraction process for dataset testing is similar to the feature extraction of the training dataset at step 6.
9. Classification using the Support Vector Machine (SVM) [28], Evaluate performance with a percentage of accuracy.

2.5. Cross-validation

Cross-validation uses k-fold cross-validation with k=10. Cross-validation divides the data into ten parts with the same number of each part. Nine parts for training and apart for validation. Then select another part as validation and nine other parts as training, and so on [29]. The full scheme of cross-validation is shown in Figure 11.

Figure 11. 10-Fold cross validation scheme

the performance measure of cross-validation used is a linear loss. A linear loss is shown in (6)

$$L = \frac{\sum_j -w_j y_j f_j}{\sum_j w_j} \quad (6)$$

herewith w_j = weight for observation j; y_j = response j ; f_j = classification score

3. Results and Discussion

The experiment performed on single GPU Core i7 7700, MSI Z270 a pro, GTX 1060 6 GB D5 amp, DDR4 16 GB, PSU 550 w and SSD 60 GB Golden Memory. Experiment scenarios are needed to get optimal measurement results. Experiment scenario as follows:

1. Data is divided into 2, training data and testing data. Selection of training data and testing data is done randomly. Experiment using AlexNet, VGG16, VGG19, ResNet50, and GoogLeNet. Classification method using SVM as described in the implementation section.
2. Comparison of accuracy results using classification methods include Support Vector Machine (SVM), k-Nearest Neighbor (k-NN), Naïve Bayes Classifier (NBC), Discriminant Analysis, and Decision Tree. Training data that used for the experiment is 70, testing data is 30.
3. Comparison of linear loss cross validation on second scenario.

The results of the 1st scenario is shown in Table 1. The experiment was carried out with the number of training and testing data varied. Accuracy is between 90% and 100%. The best average accuracy used VGG19 97.22%.

Furthermore, the 2nd scenario using the classification methods such as SVM, k-Nearest Neighbor, Naïve Bayes Classifier, Discriminant analysis and Decision Tree. It's also compared CNN models. The results show the highest accuracy was obtained using the VGG16+SVM, VGG19+kNN, and ResNet50+ SVM. Accuracy up to 100%. The result of the 2nd scenario shows in Table 2.

The 3rd scenario is a validation of accuracy in Validation is carried out on testing data using the classification method. Validation using linear loss 10-fold cross-validation. Table 3 shows the linear loss is 0-26.67%.

Table 1. A Classification Accuracy Using SVM

Experiment no.	Training Data	Testing Data	CNN model				
			AlexNet	VGG16	VGG19	ResNet50	GoogLeNet
1	70	30	96.67	100	96.67	100	96.67
2	80	20	95	90	95	100	90
3	90	10	90	100	100	90	90
average			93.89	95.56	97.22	95.56	91.11

Table 2. Comparison of Accuracy Performance between CNN Model

Classification Method	CNN Model				
	AlexNet	VGG16	VGG19	ResNet50	GoogLeNet
SVM	96.67	100	96.67	100	96.67
k-NN	90	96.67	100	96.67	96.67
Naïve Bayes	93.33	-	-	96.67	90
Discriminant Analysis	93.33	-	-	93.33	93.33
Decision Tree	96.67	93.33	93.33	90	93.33

Table 3. Linear Loss Cross-validation

Classification Method	CNN Model				
	AlexNet	VGG16	VGG19	ResNet50	GoogLeNet
SVM	3.33	6.67	13.33	3.33	3.33
kNN	10	0	3.33	0	6.67
Naïve Bayes	13.33	-	-	3.33	10
Discriminant analysis	13.33	-	-	3.33	16.67
Decision Tree	16.67	26.67	3	3.67	10

The results show the factors that influence the percentage of classification accuracy are the number of data training & testing, the classification method and the CNN model. While the factors that influence the results of linear loss are the classification method and the CNN model. The best CNN model in this experiment is ResNet50. The optimal accuracy using SVM classification method. The optimal linear loss is using k-NN.

The experiment needs to find out the differences of the result study with previous studies. In the previous study, Image size used for the training and testing phase between 128x128 pixels to 1272x1272 pixels. The number of classes classified is two and five classes. Layers that are used for CNN are 21, 22 and 45. This research is carried out in two classes of the fundus image. The image size used for the classification process is 227x227 pixels according to the default input layer on Alexnet. The number of layers used for CNN is 25. The results are shown in Table 4.

Table 4. Comparison of Classification Fundus Research using CNN

Authors	Classes	Size of images	Layers	Processing Unit	Accuracy.
Pratt et al., [11]	5 classes	512x512	45	GPU	75
Lee et al. [12]	2 classes	-	21	GPU	87.63 – 93.45
Takahashi et al. [13]	2 classes	1272x1272	22	GPU	81
Lam et al. [14]	5 classes	128x128	22	GPU	74 – 96
Proposed method	2 classes	227x227	25	GPU	90 – 100

4. Conclusion

Classification of two fundus classes is normal and neovascularization has been carried out. Experiment using CNN models are AlexNet, VGG16, VGG19, ResNet50, and GoogleNet. Classification method using Support Vector Machine, Naïve Bayes, k-Nearest Neighbor, Discriminant Analysis, and Decision Tree. The results of the experiment showed an accuracy of 90-100% with loss cross-validation of 0-26.67%.

For further work, we can create our CNN models. Measurement results can be compared with existing CNN models.

Acknowledgments

We would like to acknowledge the Ministry of Research, Technology and Higher Education, Indonesia for funding this research. We also thanks to MESSIDOR and Retinal Image Bank dataset as experiment data.

References

[1] Nentwich M.M, Ulbig M.W. Diabetic Retinopathy- Ocular Complications of Diabetes Mellitus. *World Journal of Diabetes*. 2012; 6(3): 489–499.

[2] Mathur R, Bhaskaran K, Edwards E, Lee H, Chaturvedi N, Smeeth L, Douglas I. Population trends in the 10-year incidence and prevalence of diabetic retinopathy in the UK: A cohort study in the Clinical Practice Research Datalink 2004-2014. *BMJ Open*. 2017; 7(2): 1–11.

[3] Sivaprasad S, Gupta B, Crosby-nwaobi R, Evans J. Public Health And The Eye Prevalence of Diabetic Retinopathy in Various Ethnic Groups : A Worldwide Perspective. *Surv Ophthalmol,* Elsevier Inc. 2012; 57(4): 347–70.

[4] Novita H, Moestijab. Optical Coherence Tomography (OCT). *Indonesian Ophhalmology Journal*. 2008; 6(3): 169–177.

[5] Ilyas S. Basics of Examination Technique in Eye Disease. 4th ed. Jakarta: Medical Faculty. University of Indonesia; 2012.

[6] Jelinek H.F, Cree M.J, Leandro J.J.G, Soares J.V.B, Cesar R.M, Luckie A. Automated Segmentation Of Retinal Blood Vessels And Identification Of Proliferative Diabetic Retinopathy. *J Opt Soc Am A Opt Image Sci Vis*. 2007; 24(5): 1448–56.

[7] Goatman K.A, Fleming A.D, Philip S, Williams G.J, Olson J.A, Sharp P.F. Detection of New Vessels On The Optic Disc Using Retinal Photographs. *IEEE Trans Med Imaging*. 2011; 30(4): 972–9.

[8] Akram MU, Khalid S, Tariq A, Javed MY. Detection of neovascularization in retinal images using multivariate m-Mediods based classifier. *Comput Med Imaging Graph, Elsevier Ltd*. 2013; 37(5-6): 346-357. Available from: http://dx.doi.org/10.1016/j.compmedimag.2013.06.008.

[9] Welikala R.A, Fraz M.M, Dehmeshki J, Hoppe A, Tah V, Mann S, Williamson T.H, Barman S.A. Computerized Medical Imaging and Graphics Genetic Algorithm Based Feature Selection Combined

With Dual Classification For The Automated Detection Of Proliferative Diabetic Retinopathy. *Comput Med Imaging Graph*, *Elsevier Ltd*. 2015; 43: 64–77.
[10] Gupta G, Kulasekaran S, Ram K, Joshi N, Sivaprakasam M, Gandhi R. Computerized Medical Imaging and Graphics Local characterization of neovascularization and identification of proliferative diabetic retinopathy in retinal fundus images. *Comput Med Imaging Graph, Elsevier Ltd*. 2017; 55: 124–32.
[11] Pratt H, Coenen F, Broadbent D.M, Harding S.P, Zheng Y. *Convolutional Neural Networks for Diabetic Retinopathy*. Procedia Comput Sci MIUA (2016): 1–6.
[12] Lee C.S, Baughman D.M, and Lee A.Y. Deep Learning Is Effective for the Classification of OCT Images of Normal versus Age-Related Macular Degeneration. *Ophthamol. Retina.* 2016; 1: 322–327.
[13] Takahashi H, Tampo H, Arai Y, Inoue Y, Kawashima H. Applying artifial Intelligence to disease staging : Deep learning for improved staging of Diabetic Retinopathy. *PLoS ONE*. 2017; 12(6): e0179790.
[14] Lam C, Yu C, Huang L, Rubin D. Retinal lesion detection with deep learning using image patches. *Invest Ophthalmol Vis Sci*. 2018; 59: 590-596.
[15] Deng L, Yu D. Deep Learning Method and Application. Redmond, Washington : Now Publisher. 2014: 6-7.
[16] Wang R, Zhang J, Dong W, Yu J, Xie C.J, Li R, Chen T, Chen H. A Crop Pests Image Classification Algorithm Based on Deep Convolutional Neural Network. *TELKOMNIKA Telecommunication Computing Electronics and Control*. 2017; 15 (3): 1239–1246.
[17] Baharin A, Abdullah A, Yousoff S N M. Prediction of Bioprocess Production Using Deep Neural Network Method, *TELKOMNIKA Telecommunication Computing Electronics and Control.* 2017; 15(2): 805–813.
[18] Krizhevsky A, Sutskever I, Hinton G*. Imagenet classification with deep convolutional neural networks*. Advances in Neural Information Processing Systems 25. 2012.
[19] Wang C, Xi Y. Convolutional Neural Network for Image Classification. Johns Hopkins University Baltimore, MD 21218, cs.jhu: ~cwang107.
[20] Dumoulin V, Visin F. *A guide to convolution arithmetic for deep learning*. Université de Montréal & Politecnico di Milano. 2018: 8-15.
[21] Nagi J, Ducatelle F, Di Caro G, Ciresan D, Meier U, Giusti A, Nagi F, Schmidhuber J, and Gambardella L. *Max-pooling convolutional neural networks for vision-based hand gesture recognition*. In Proceedings of the IEEE International Conference on Signal and Image Processing Applications. 2011; 342–347.
[22] Sainath T.N, Vinyals O, Senior A, Sak H. *Convolutional, long short-term memory, fully connected deep neural networks*. In ICASSP. 2015.
[23] Wu H, Gu X. Towards dropout training for convolutional neural networks. *Neural Networks.* 2015; 71: 1–10.
[24] Simonyan K, Zisserman A. Very Deep Convolutional Networks for Large-Scale Image Recognition. 2014;1–14. Available from: http://arxiv.org/abs/1409.1556
[25] He K, Sun J. Deep Residual Learning for Image Recognition. 2015; 1–9. Available from : https://www.cv-foundation.org/openaccess/content_cvpr_2016/papers/He_Deep_Residual_LearningVPR_2016_paper.pdf.
[26] Szegedy C, Liu W, Jia Y, Sermanet P, Reed S, Anguelov D, et al. Going Deeper with Convolutions. 2014; 1–9. Available from : https://www.cs.unc.edu/~wliu/papers/GoogLeNet.pdf.
[27] Decencière E, Zhang X, Cazuguel G, Lay B, Cochener B, Trone C, Gain P, Ordonez R, Massin P, Erginay A, Charton B, Klein JC. Feedback On A Publicly Distributed Image Database: The Messidor Database. *Image Analysis and Stereology.* 2014; 33(3): 231-234.
[28] Manning C.D, Raghavan P, Schütze H. Introduction to Information Retrieval Introduction. *Computational Linguistics*. 2008; 35: 234-264.
[29] Dudoit S. Loss-Based Estimation with Cross-Validation : Applications to Microarray Data Analysis and Motif Finding. *Biostatistics*. 2003; 5(2): 56–68.